CIMAC CONGRESS 25
ZURICH, MAY 19 – 23, 2025

2025 | 455

The steady-state and transient performance of an ammonia-diesel dual fuel multi-cylinder engine

Fuels - Alternative & New Fuels

Longfei Deng, Tianjin University

Caifeng Hao, China North Engine Research Institute
Zhenyuan Zi, Tianjin University
Binyang Wu, Tianjin University

ABSTRACT

The utilization of ammonia as carbon-free fuels holds significant potential for various applications in energy systems. To enhance the ammonia-diesel dual-fuel engine performance, it is necessary to blend a highly reactive fuel due to its inherent difficulty in igniting and lower combustion speed. The study is conducted on an inline six-cylinder heavy-duty ammonia-diesel dual fuel engine with a displacement of 13 liters, where the ammonia was injected into manifold using low-pressure injection and direct injection of diesel into the cylinders. Initially, we investigated the effects of ammonia energy ratio and diesel injection strategies on economy and emission of ammonia-diesel dual-fuel engine under steady-state (WHSC) conditions to optimize its power and emission performance. The research findings demonstrated that while maintaining the original engine's power and torque levels, the maximum substitution ratio of ammonia reached 59%, resulting in an effective thermal efficiency of 48.5%, which was 3% higher than that of the original engine. Moreover, both NOx and NH3 emissions were 0.089 g/kWh and 0.62 ppm, respectively. Based on the steady-state research results, the effects of ammonia energy ratio and urea injection strategy on the power and emission performance of an ammonia-diesel dual-fuel engine were investigated. Compared with the original engine, the research results showied a reduction in cycle fuel consumption by 2% along with an achieved ammonia substitution ratio reaching up to 53%. After treatment, NOx emissions stood at 0.22 g/kWh while NH3 emissions measured at only 7.18 ppm. Furthermore, all other pollutant emissions from both steady-state and transient operations met China's sixth-stage emission requirements, which provides a significant reference for the commercial application of an ammonia-diesel engine.

1 Introduction

Over the years, global warming caused by greenhouse gases has led to an increase of approximately 0.87°C in the global average temperature from 2006 and 2015 compared to pre-industrial levels[1, 2], with some regions experiencing temperature increases exceeding 1.5°C [3]. As a result, governments and organizations worldwide are actively working to mitigate greenhouse gas emissions (GHG) [4, 5]. In 2019, carbon dioxide (CO_2) accounted for 64% of global greenhouse gas emissions, making it the largest portion of emissions, with the transportation sector contributing about 15%, which should be concern in significance[6-9]. In China, from 2000 to 2020, greenhouse gas emissions have increased by about 1.5 times[10, 11]. The transportation sector in China accounted for around 10% of the total greenhouse gas emissions[1]. Statistics show that 60% of CO_2 emissions in China's road transport come from 63 million medium- and heavy-duty trucks[12]. However, based on current data, heavy-duty internal combustion engines will undoubtedly continue to dominate the road and marine transport sectors in the future[13]. Even by 2040, internal combustion engines are expected to remain the primary power source in the transportation sector. Therefore, actively seeking efficient, clean combustion technologies and reliable alternative fuels is an important path toward achieving carbon neutrality in internal combustion engines[14].

Among various alternative fuels, hydrogen, although a zero-carbon fuel with relatively simple combustion products, has a much higher storage and transport cost compared to ammonia. In most cases, the cost of hydrogen storage is 26 to 30 times higher than that of ammonia storage [15]. Ammonia, with an annual production of 180 million tons, is the second most commercially produced chemical in the world[16, 17]. As a result, various large-scale infrastructures, such as major ports, distribution pipelines, medium-sized distributors, and small users, can rapidly implement ammonia-based economies to support the future ammonia economy[18]. Ammonia can be produced conveniently from fossil fuels, nuclear energy, solar energy, etc. [19]. In the future, the ammonia synthesis industry could achieve zero-carbon production at a cost lower than conventional ammonia [20]. Therefore, ammonia can serve as a renewable energy carrier [21-24], making it a clean alternative fuel for internal combustion engines[17].

The maximum laminar flame speed of ammonia/air premixed flames at different equivalence ratios is approximately 7 cm/s [25-30], which is about one-fifth of that of methane (CH_4) [27]. Due to the low combustion speed of NH_3/air flames, flame enhancement becomes crucial for the successful application of ammonia as a fuel [24, 31]. Diesel is often chosen as a high-activity fuel to enhance the flammability of ammonia[11, 32]. Direct injection of liquid ammonia mixed with diesel has brought higher ammonia substitution rates and considerable thermal efficiency to compression ignition (CI) engines under low load conditions[33]. Moreover, the overlapping injection of liquid ammonia and diesel can achieve the highest co-combustion efficiency and the lowest emissions[34]. Jin et al. [35] experimentally studied the impact of diesel injection strategies and ammonia energy replacement (AER) on the combustion process and emissions when ammonia is injected into the intake manifold. When a single diesel injection is used, as AER increases from 0% to 90%, the indicated thermal efficiency (ITEg) continuously decreases, and N_2O emissions worsen, negatively affecting GHG reduction. However, by using double injections to improve the in-cylinder combustible mixture activity and increase the combustion rate, unburned ammonia emissions and incomplete combustion losses can be reduced. Ultimately, with a 50% AER, they achieved a 49.18% ITEg and a 14.2% reduction in GHG emissions under this operating condition. Using a premixed compression ignition mode under low-load conditions not only yields high ITEg but also offers a win-win situation against ammonia escape and GHG emissions reduction[36]. Pei et al.[37] supported this conclusion, showing that under low-load conditions, ITEg could be further improved to 51.5%. As the ammonia substitution ratio increases, particulate matter emissions transition from aggregated to nucleated particle forms, with nucleated particles exceeding 60% as the injection timing is advanced [38]. Similarly, Shin et al.[39] showed that premixed combustion could compensate for the low

combustion speed of ammonia while improving engine thermal efficiency. Liu et al.[40] found that at 25% load and with a diesel injection pressure of 130 MPa, when the ammonia substitution ratio increased to 60%, the Cov_{IMEP} (Coefficient of Variation of Indicated Mean Effective Pressure) initially decreased and then increased significantly to over 5%[41]. However, when the substitution ratio was maintained at 40%, the Cov_{IMEP} decreased with increasing injection pressure. Wang et al.[42] showed in their study on ammonia-diesel dual-fuel engines with a wide range of ammonia substitution ratios that the engine's Cov_{IMEP} could be kept within 3%. During testing, Yousefi et al.[22] found that adjusting the injection strategy is constrained by Cov_{IMEP}. Under high-load conditions, where the engine cannot operate in premixed combustion mode due to limited in-cylinder peak pressure, appropriate exhaust gas recirculation (EGR) can be used to reduce emissions and extend the load range[43].

In summary, although many scholars have made significant progress in the fields of ammonia combustion, ammonia-diesel engine combustion strategies, pollutant generation and consumption mechanisms, and cyclic variation, there is limited research on commercial heavy-duty multicylinder engines under WHSC and WHTC conditions. Therefore, it remains uncertain whether ammonia can be used as a fuel for heavy-duty commercial vehicles operating under highly variable operating conditions. Furthermore, due to the uniqueness of ammonia-diesel engine fuel and original emissions, the mechanisms of synergistically controlling the in-cylinder combustion process and aftertreatment system strategies still need further investigation.

The present study systematically investigates the effects of ammonia energy replacement (AER) and diesel injection strategies on combustion and original emission performance under WHSC conditions for ammonia-diesel multicylinder engines. Building on the optimization results from WHSC, this study further explores the impact of AER and aftertreatment urea injection strategies on the power and emission performance under WHTC conditions, revealing the technological pathway for achieving efficient and clean operation of ammonia-diesel engines. This research provides a theoretical foundation for the further commercialization of ammonia-diesel engines.

2 EXPERIMENTAL DETAILS

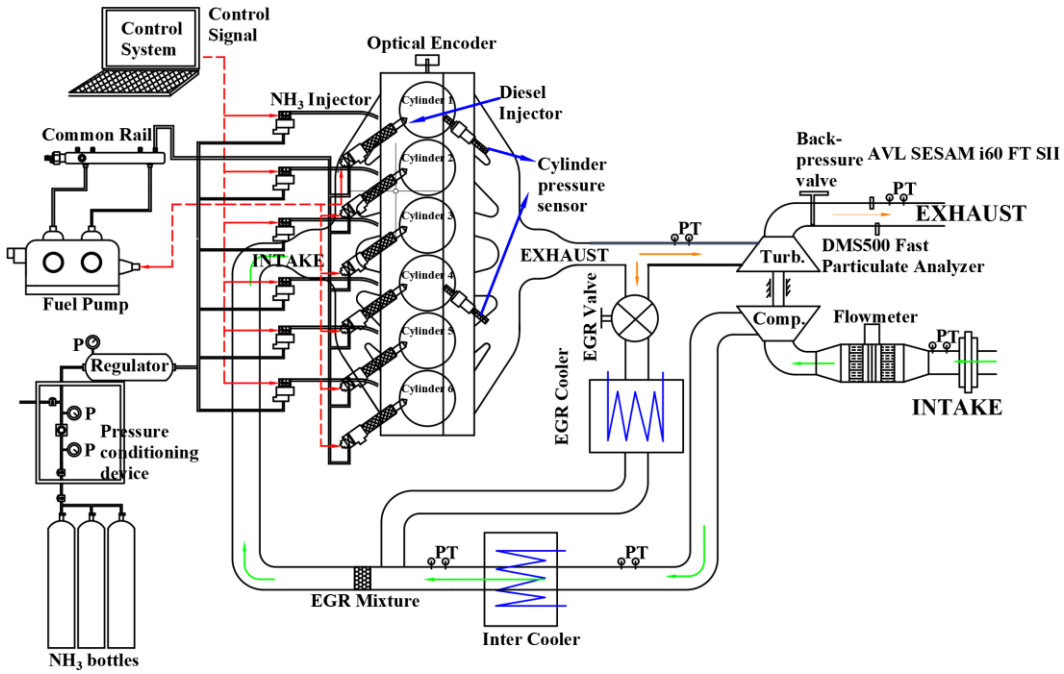

Fig. 1 Schematic of the experimental setup

Table 1 Engine specifications

Item	Value
Bore × stroke	127 mm × 165 mm
Rated Power/Speed	1
Compression ratio	19:1
Injection system	Common rail
Maximum rail pressure	180 MPa
Ammonia injection method	Intake manifold injection
Ammonia injection pressure (bar)	7~8
Nozzle number×diameter (mm)	8×0.169

The experiment about the research was conducted on an inline six-cylinder heavy-duty ammonia-diesel dual fuel (ADDF) engine, which was modified on the basis of a diesel engine manufactured by Weichai Power Co., LTD. Figure 1 shows the schematic of the test system. The test system is equipped high-pressure common rail system with a maximum injection pressure of 180 MPa with the third-generation Bosch. The schematic of ammonia supply system for this experiment is shown in Figure 1. Ammonia is injected through a multi-point injection system in the intake manifold during the intake valve opening period. The ammonia is supplied from a steel cylinder, with a pressure regulator tank added after the ammonia cylinder to stabilize the supply pressure between 7 bar and 8 bar, thus allowing more precise control of the ammonia supply pressure. An ammonia flow meter is installed after the pressure regulator tank, and the ammonia is supplied to the ammonia gas rail via the flow meter. Six ammonia injectors are arranged along the gas rail to supply ammonia to each of the six cylinders. For the remaining intake and exhaust system of the test engine, all components, except for the intercooler, remain unchanged from the original configuration in order to verify the feasibility of the engine with minimal modifications.

2.1 Emission Testing Equipment

Table 2 Measurement accuracy of instruments

Measurements	Instruments	Accuracy
Combustion measurement systems	IndiMicro 602	± 0.3 %
In-cylinder pressure	Kstler 6125C	≤±0.4 bar
Air mass flow	FMT700-P	±1 %
Ammonia mass flow	DET8623	±0.35 %
Fuel flow meter	AVL 735S+753C	0.12 %
NH_3, NO, NO_2, N_2O and so on	AVL SESAM i60 FT SII	±1%
	Sensitivity of DMS 500 (RMS at 1 Hz)	
	10 nm	1.0×10^3 (dN/dlogDp /cc)
	30 nm	4.0×10^2 (dN/dlogDp /cc)
	100 nm	1.7×10^2 (dN/dlogDp /cc)
	300 nm	8.0×10^1 (dN/dlogDp /cc)

The in-cylinder pressure is measured by a Kistler 6125C, using the AVL IndiMicro 602 to record the in-cylinder pressure for combustion analyzing. The diesel and ammonia consumption were measured by an AVL 735S+753C and DET8623, respectively. Ammonia (NH_3), nitric oxide (NO), nitrogen dioxide (NO_2), nitrous oxide (N_2O), carbon monoxide (CO) and carbon dioxide (CO_2) emissions were measured by a Fourier transform infrared spectrometer (AVL SESAM i60 FT SII). The analyzer consists of a Fourier transform

infrared absorption spectrometer for the detection of various exhaust gas components. PM emissions are measured by Cambustion DMS 500, which classifies the particulate size according to the electric mobility. It can also test the particulate size distribution, quantity, and quality information of particulates with a diameter of 5 to 1000 nm. The T10-90% response time is 200 ms, and the highest sampling frequency is 10 Hz. The measurement accuracies of the acquisition instruments used in the experiment were shown in Table 2.

2.2 The operating conditions and structure of aftertreatment system

The World Harmonized Stationary Cycle (WHSC) operating conditions are calculated based on the engine's external characteristics. Before implementing the WHSC experiments, an initial external characteristic assessment was carried out, and the parameters for each WHSC operating point were then calculated based on this. The specific parameters are shown in Table 3. The aftertreatment system is a technological means to effectively reduce pollutant emission concentrations to meet increasingly stringent emission regulations. To reduce emissions from the ammonia-diesel dual-fuel engine and meet China's Stage 6 vehicle emission standards, we integrated the aftertreatment system into the exhaust system to study the internal and external collaborative purification method. The aftertreatment system consists of three stages of selective catalytic reduction (SCR), two stages of ammonia selective catalytic reduction (ASC), along with diesel oxidation catalyst (DOC) and diesel particulate filter (DPF). The detailed structure is shown in Figure 2.

Table 3 Parameters of WHSC Operation conditions

Operation conditions	Speed /(r/min)	Torque /Nm	Running time / s
1	600	0	210
2	1255	2300	50
3	1255	575	250
4	1255	1610	75
5	1017	2300	50
6	898	561	200
7	1136	1610	75
8	1136	575	150
9	1255	1150	125
10	1493	2188	50
11	1017	1150	200
12	1017	575	250
13	600	0	210
Total	-	-	1895

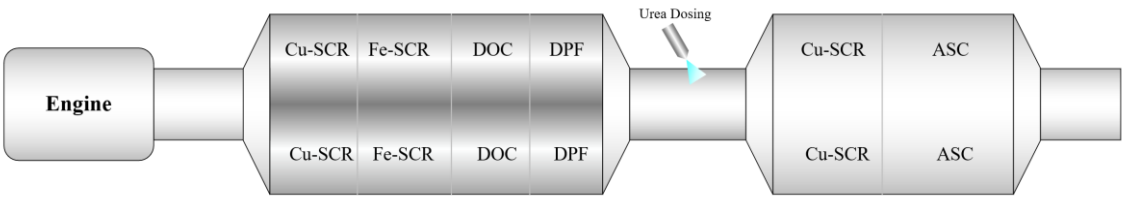

Fig. 2 The structure of aftertreatment system

3 THE STEADY-STATE EXPERIMENT RESEARCH

Our research team conducted a systematic study on the combustion and emission performance of ammonia-diesel engines using a multi-cylinder to single-cylinder engine setup in previous work[31, 32, 35-37, 43]. The results showed that under medium and low loads, a pre-mixed compression ignition mode could be used, while at high loads, a diesel ignition mode limited by knocking pressure was more effective, achieving excellent performance in terms of power, economy, and emissions. Since the engine used in this study differs from the ones in the aforementioned research, the parameters from those studies cannot be directly applied to this one. However, the fundamental trends remain consistent, and therefore, this study conducted a validation experiment based on these findings. The main focus was on the ammonia energy substitution rate and the effect of diesel injection strategies on engine performance and emissions. Figure 3 shows the cylinder pressure and heat release rate (HRR) at different load rates, Figure 4 shows the emissions and brake thermal efficiency (BTE) at different load rates, and Figure 5 illustrates the changes in combustion phase and the length of each combustion stage at different load rates.

25% load was firstly conducted, with the pre-injection timing set at -40° CA ATDC (After Top Dead Center). The pre-injection fuel amount was increased from 5 mg/cycle to 19.4 mg/cycle. As shown in Figure 3, the increase in pre-injection fuel amount slightly raised the peak in-cylinder pressure while significantly advanced the initial heat release timing. Additionally, the peak HRR was suppressed, which extended the combustion duration and effectively increased the in-cylinder thermal environment, thus promoting ammonia combustion. As a result, the unburned ammonia emission dropped significantly from 56.82 g/(kW·h) to 8.37 g/(kW·h), while NO emission slightly increased from 8.68 g/(kW·h) to 10.76 g/(kW·h).

For case 3 and case 4, the pre-injection timing was advanced from -40° CA ATDC to -45° CA ATDC. From Figures 3, 4, and 5, it can be observed that further advancing the injection timing had little effect on emissions, but it worsened thermal efficiency. Therefore, for low-load conditions, a pre-injection timing around -40° CA ATDC is a more appropriate injection strategy.

For case 3, the actual ammonia energy substitution rate was 63%, at which point all of the diesel fuel was injected during the pre-injection phase. If the ammonia energy proportion were to be further increased, it would not be possible to inject enough diesel during the pre-injection phase to establish a good in-cylinder thermal environment and fuel reactivity. Therefore, at 25% load, the maximum ammonia energy substitution rate is around 63%.

At 50% load, compared to case 5, case 6 increased the injection pressure from 85 MPa to 100 MPa. The increase in rail pressure promoted fuel atomization and evaporation, which advanced the combustion phase. As shown in Figure 3, this caused a sawtooth pattern in the cylinder pressure, indicating that the combustion was violent at this point. Based on this, during the experiment, the injection amount was reduced to suppress the formation of combustible mixtures in the early phase, thus mitigating the issue of violent combustion. Ultimately, it was found that at this load, an SOI (Start of Injection) of -42° CA ATDC, combined with a pre-injection amount of 20 mg/cycle, provided a good compromise between thermal efficiency and emissions. On this basis, the optimal ammonia energy substitution rate at 50% load was studied. The results indicated that with a 62% energy substitution rate, thermal efficiency could be improved without significantly increasing emissions. At this point, the NO emission and NH_3 emission rates were roughly equivalent.

At 70% load, the ammonia energy substitution rate was increased from 43% to 60%, resulting in an increasing trend in BTE, which peaked at 48.1% when the ammonia energy substitution rate reached 60%. As shown in Figure 3, with the diesel injection timing kept unchanged, the increase in ammonia energy substitution rate was accompanied by a reduction in the main diesel injection amount. Under constant pre-mixed fuel reactivity, combustion phase delay could be achieved at

an appropriate substitution rate, resulting in improved emissions performance and fuel economy.

In figure 3, case 13 and case 14 show the changes in-cylinder pressure and heat release rate under 100% load when the injection timing was adjusted. The main injection timing was advanced from -7° CA ATDC to -11° CA ATDC. As shown in Fig. 4, ammonia slip decreased by about 5 g/(kW·h), and NOx emissions were approximately 12 g/(kW·h). However, due to the limitations of in-cylinder peak pressure, it was not possible to further advance the main injection timing, nor could a dual injection strategy be adopted. Therefore, at full load, ammonia slip remained relatively high.

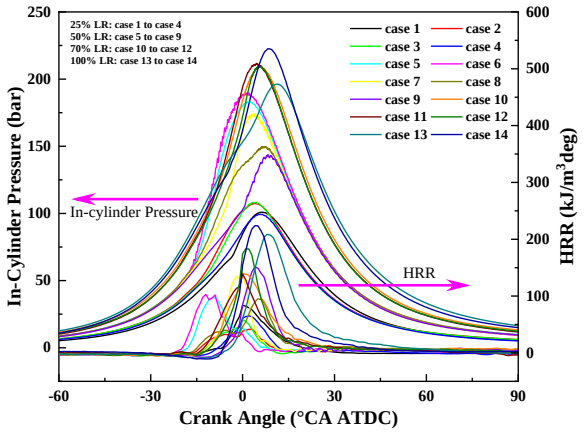

Fig. 3. The In-cylinder pressure and HRR of different load ratio

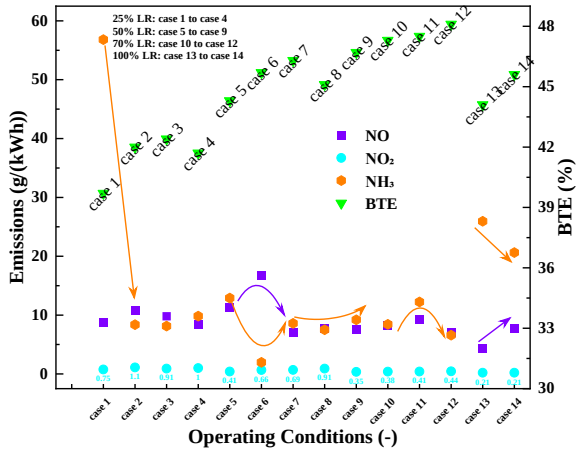

Fig. 4 The critical emissions and BTE of ADDF engine under different load ratio

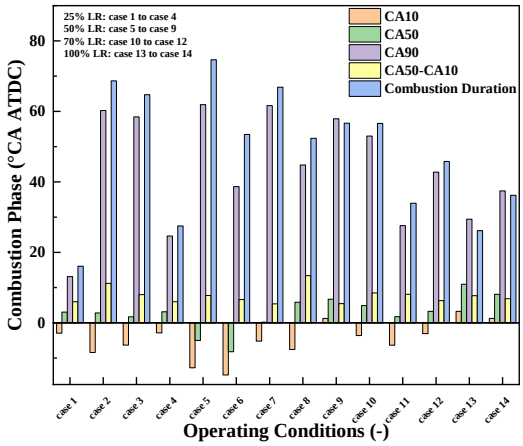

Fig. 5 The combustion phase of ADDF under different load ratio

3.1 The optimization of ammonia energy ration and performance under WHSC

To conduct the WHTC test, it is necessary to first perform the WHSC test to calibrate and optimize engine performance across the full operating range. Figure 6 shows the optimized ammonia energy substitution rate for each WHSC operating condition. At idle conditions, due to the poor in-cylinder thermodynamic environment, the addition of ammonia leads to significant engine speed fluctuations and instability, so pure diesel mode is adopted. As the engine speed and load increase, both the in-cylinder temperature and pressure continuously rise, and the increasing total diesel injection amount in the cylinder provides the foundation for adopting a more flexible diesel injection strategy. This allows for controlling the ignition conditions of the mixture by adjusting the injection strategy. Ultimately, through the optimization of the combustion strategy, the ammonia-diesel multi-cylinder engine can operate stably at more than 50% ammonia energy substitution ratio under non-idle conditions. In the medium-to-high load range, the maximum ammonia energy substitution ratio reached 69%.

Figure 7 shows the fuel consumption rate distribution under the WHSC conditions. The fuel consumption rate is calculated by converting the ammonia energy into an equivalent amount of diesel fuel. It can be observed that as the engine torque increases, the fuel consumption rate initially decreases and then increases. Meanwhile, as the engine speed increases, the fuel consumption rate shows an increasing trend. Under steady-state conditions, the lowest fuel consumption was obtained at a speed of 1255 r/min and a torque of 1610 N·m, with a value of 172.6 g/(kW·h).

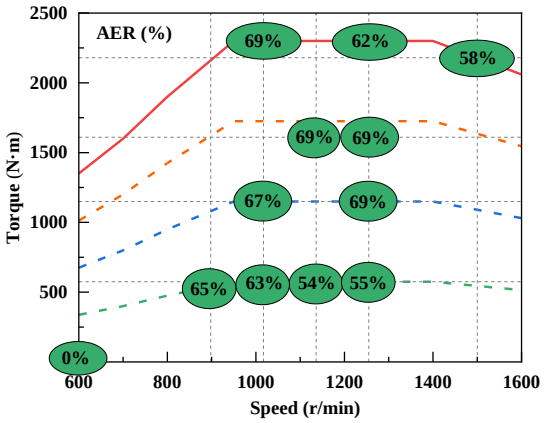

Fig. 6 Amonia energy ratio of WHSC

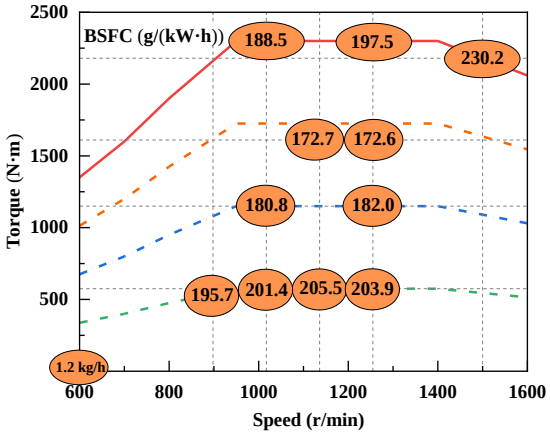

Fig. 7 Fuel consumption of WHSC

3.2 The emissions performance optimization under WHSC

Figure 8 shows the BTE under pure diesel mode and ammonia-diesel dual-fuel mode at steady-state conditions in the WHSC. Compared to pure diesel mode, the BTE of the ammonia-diesel engine is generally lower at low torque conditions. This is primarily due to the relatively poor thermodynamic environment at these conditions, along with the high ammonia energy substitution ratio, which is not conducive to the complete combustion of the in-cylinder mixed fuel. As the load increases, the in-cylinder combustion conditions are significantly optimized, and the advantages of high fuel premixing in the ammonia-diesel dual-fuel (ADDF) mode are realized. This reduces the gap in effective thermal efficiency between the dual-fuel mode and pure diesel mode. At engine speeds of 1136 r/min and 1255 r/min with a torque of 1610 N·m, the ADDF mode achieves the highest BTE, both at 48.8%, which is 3.0% and 3.1% higher than the pure diesel mode, respectively. This is mainly due to the higher heat release rate and faster combustion rate under this condition.

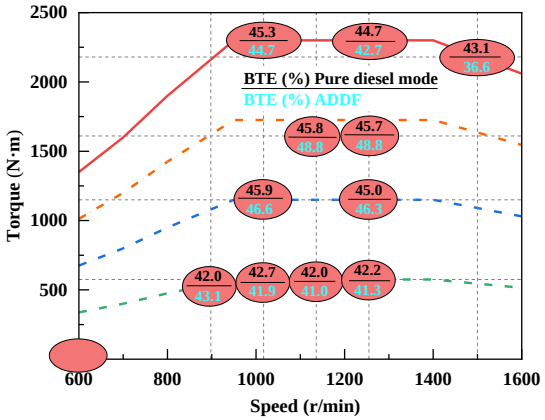

Fig. 8 BTE of amonia-diesel dual fuel mode and pure diesel mode under the WHSC

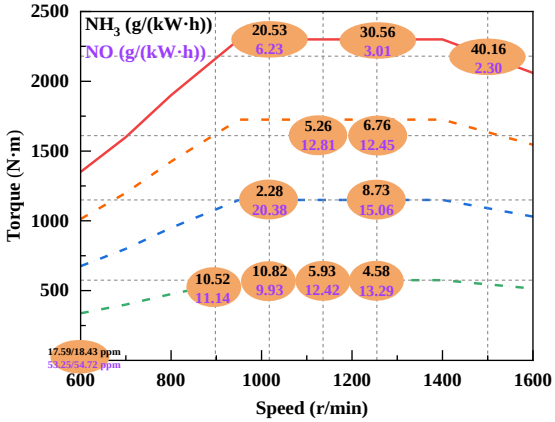

Fig. 9 NH_3 emission of ammonia-diesel fual fuel mode under the WHSC

Figures 9 and 10 show ammonia slip, NO, NO_2, and N_2O emissions at each WHSC operating conditions. From the figures, it can be observed that the region with low unburned ammonia emissions is mainly concentrated in the medium-to-high torque range. Through optimization of the air and combustion systems, unburned ammonia emissions can be reduced to as low as 2.28 g/(kW·h). It is worth noting that at full load, unburned ammonia emissions are excessively high, reaching up to 40.16 g/(kW·h). This is consistent with the research results from the research group[36, 43] and previous multi-cylinder engine tests, which indicate that at full load, the engine is limited by knocking pressure, making it difficult to optimize the combustion of ammonia-diesel mixtures through methods like adjusting diesel injection strategies, resulting in higher ammonia emissions.

With the ammonia as fuel to inject into the cylinder complicates the formation and evolution pathways of NO and NO_2 in the engine cylinder[44]. On one hand, ammonia combustion generates NO and NO_2; on the other hand, at high temperatures, ammonia's thermal denitrification reaction of ammonia suppresses the formation of NO and NO_2. As shown in Fig. 9, NO shows an overall trend of first increasing and then decreasing as engine torque increases. In steady-state conditions, the low NO emission region is also concentrated in the full load range, where, on one hand, the in-cylinder temperature is high, and on the other hand, there is a large amount of unburned ammonia, providing favorable conditions for the thermal denitrification process. When the engine speed is 1493 r/min and the torque is 2188 N·m, NO emissions reach their lowest point, at 2.30 g/(kW·h). NO_2 emissions decrease as engine torque increases, with the minimum value being 0.20 g/(kW·h).

Compared to traditional diesel engines, ADDF engines emit higher levels of N_2O, which has a much greater impact on the greenhouse effect than carbon dioxide (CO_2) and requires special attention. N_2O is mainly generated in large amounts in the low-temperature regions, but as engine torque increases, the combustion conditions in the cylinder improve, the combustion temperature rises, and the high-temperature region in the cylinder becomes more widespread, which helps reduce N_2O emissions. However, as the engine speed increases, N_2O generally shows an increasing trend. This is primarily due to the increase in engine intake air, which, to some extent, lowers the in-cylinder combustion temperature and promotes N_2O formation. When the engine speed is 1017 r/min and the torque is 1150 N·m, N_2O emissions are at their lowest, at 0.11 g/(kW·h). The adoption of the ADDF mode reduces the carbon in the fuel, leading to a reduction in CO_2 emissions under the same operating conditions. However, due to the high greenhouse effect of N_2O, the overall greenhouse gas emissions from the engine are primarily dominated by N_2O emissions. Comparing CO_2 equivalent (CO_2eq) emissions under pure diesel mode and ammonia-diesel dual-fuel mode, it is evident that the dual-fuel mode achieves a significant reduction in CO_2eq emissions in the medium-to-high load range around 1000 r/min to 1100 r/min. Additionally, in other operating conditions, CO_2eq emissions are also reduced to varying degrees. Under steady-state testing, the CO_2eq emissions for the ADDF mode are 313.40 g/(kW·h), representing a 43.3% reduction in CO_2eq emissions compared to the pure diesel mode.

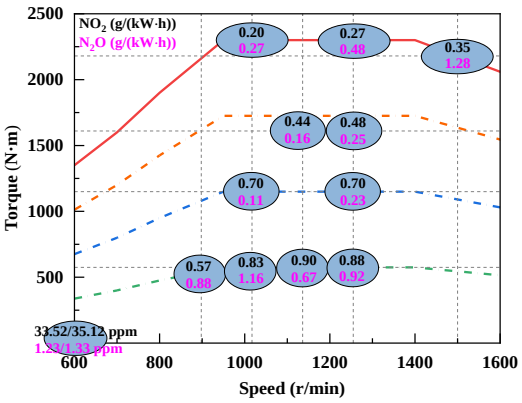

Fig. 10 NO and NO2 emissions under WHSC

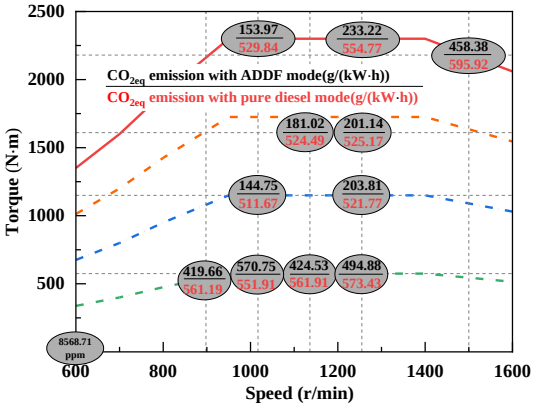

Fig. 11 CO_{2eq} emissions under WHSC

A comprehensive analysis of the performance of the ammonia-diesel multi-cylinder engine under steady-state testing shows that through the coordinated optimization of the air and combustion systems in the ADDF mode, it is possible to achieve an effective thermal efficiency comparable to that of pure diesel mode. However, in terms of emissions, the ADDF mode faces the issues of high unburned ammonia and NOx emissions. To reduce the emissions of pollutants from ammonia-diesel engines and achieve efficient and clean combustion, it is essential to match the engine with an appropriate aftertreatment system. The proper aftertreatment system will help address the challenges related to unburned ammonia and NOx emissions, thus enabling the engine to meet stringent emission standards while maintaining optimal performance.

3.3 The optimization of emissions performance at the outlet of aftertreatment system

Aftertreatment technology is an important means of achieving external purification of pollutants from engine emissions. To further reduce pollutant emissions from ammonia-diesel engines and verify the effectiveness of the engine aftertreatment system, the addition of an aftertreatment system increases the exhaust backpressure by 10 to 20 kPa, resulting in an increase in pumping losses. Figure 12 shows the changes in BTE under steady-state WHSC condition 13, both before and after the installation of the aftertreatment system. Due to the increased pumping losses, some operating conditions show a slight decrease in BTE after the addition of the aftertreatment system. However, the reduction is within an acceptable range, and the highest BTE still reaches 48.69%. Figure 13 compares the original ammonia emissions from the ammonia-diesel multi-cylinder engine with the ammonia emissions after the installation of the aftertreatment system. It can be seen that after the aftertreatment system was added, ammonia emissions at each condition in steady-state WHSC drastically decreased. At the operating condition of 1493 r/min and 2188 N·m, where ammonia emissions were originally the highest, the NH_3 emission was reduced to just 2.29 ppm, demonstrating the significant effectiveness of the aftertreatment system in reducing ammonia slip.

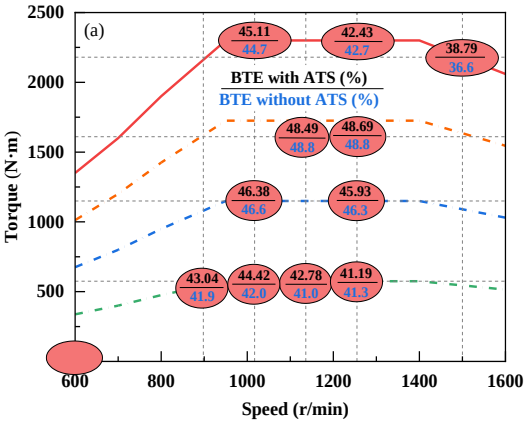

Fig. 12 BTE of WHSC conditions

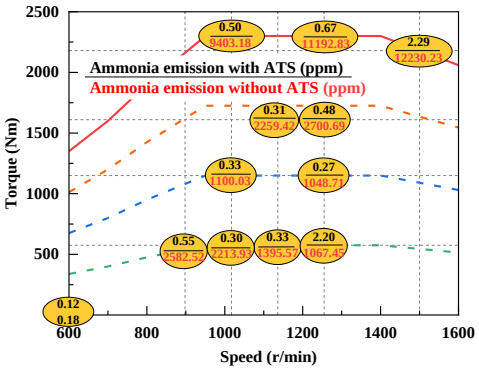

Fig. 13 Ammonia emission of WHSC conditions with and without ATS

Table 4 Comparison of CO and HC emission with after-treatment system at 13 working conditions of WHSC cycle

Operation conditions	Speed r/min	Torque N·m	Running time /s	CO ppm	CO g/(kW·h)	HC ppm	HC g/(kW·h)
1	600	0	210	0.77	-	1.9	
2	1255	2300	50	-	0.004	-	0.008
3	1255	575	250	-	0.002	-	0.020
4	1255	1610	75	-	0.003	-	0.004
5	1017	2300	50	-	0.001	-	0.003
6	898	561	200	-	0.004	-	0.007
7	1136	1610	75	-	0.002	-	0.014
8	1136	575	150	-	0.004	-	0.009
9	1255	1150	125	-	0.003	-	0.021
10	1493	2188	50	-	0.002	-	0.006
11	1017	1150	200	-	0.001	-	0.006
12	1017	575	250	-	0.006	-	0.011
13	600	0	210	0.77	-	1.9	
WHSC CO emission at ATS outlet (g/(kW·h))						0.003	
WHSC HC emission at ATS outlet (g/(kW·h))						0.011	

Carbon monoxide (CO) and unburned hydrocarbons (HC) in the exhaust are also two types of unburned emissions in ammonia-diesel engines. These emissions can be converted into water and carbon dioxide through the DOC module in the aftertreatment system, achieving the purpose of purification. Among the various emissions from ammonia-diesel engines, the proportion of CO and HC emissions is generally small. Table 4 provides a comparison of CO and HC emissions at each point under WHSC conditions, before and after the installation of the aftertreatment system. After the aftertreatment system, CO emissions are significantly

reduced. The comprehensive CO emission value after the WHSC test with the aftertreatment system is only 0.003 g/(kW·h), well below regulatory requirements. For HC emissions, the value after the WHSC test with the aftertreatment system is 0.011 g/(kW·h), indicating a substantial reduction in HC emissions as well. This demonstrates the effectiveness of the aftertreatment system in significantly lowering both CO and HC emissions, contributing to the cleaner operation of the ammonia-diesel engine.

NOx is one of the main pollutants that the aftertreatment system aims to purify. NOx and ammonia undergo a thermal denitrification reaction during in-cylinder combustion, reducing NOx to nitrogen. However, due to the limited reduction capacity of ammonia, complete in-cylinder NOx purification is difficult to achieve, which is why an SCR module is still required to further reduce NOx. Additionally, since the exhaust contains a significant amount of unburned ammonia, the ammonia will react with NOx as both pass through the SCR module, helping to reduce NOx. The presence of unburned ammonia requires adjustments to the urea injection quantity and strategy in the SCR module. Figure 14 compares the original NO and NO_2 emissions and the aftertreatment emissions under WHSC conditions, and provides the corresponding urea injection strategy for each operating condition in the SCR module. It can be observed that after the aftertreatment system, NO and NO_2 in the exhaust are nearly eliminated, with both pollutants being reduced by more than 96%. Table 4 shows the NOx emissions at each condition under WHSC conditions. After the installation of the aftertreatment system, the comprehensive NOx emission for the WHSC test is only 0.089 g/(kW·h), well below the China National VI (Euro 6) standards. Regarding the urea injection strategy, comparing it with the original ammonia emissions shows that at full load, due to the significantly higher unburned ammonia in the exhaust compared to other operating conditions, ammonia and NOx react in the SCR module during the aftertreatment phase. At this point, the ammonia-to-nitrogen ratio correction factor can be maintained within 0.30, significantly reducing the urea injection quantity at full load. However, in the 50%-75% load range, where ammonia emissions are lower, the urea injection amount increases substantially. Compared to conventional engines, the introduction of ammonia fuel reduces the urea injection quantity in the aftertreatment system, keeping the ammonia-to-nitrogen ratio correction factor below 0.90 for the ADDF engine in its main operating range. This optimization of the urea injection strategy helps to minimize the amount of urea required, further enhancing the efficiency of the aftertreatment system.

Ammonia-diesel engines still require a portion of diesel fuel to regulate the in-cylinder mixture's reactivity and ignite the low-reactivity ammonia fuel, which results in particulate matter (PM) emissions in the exhaust. The DPF module in the aftertreatment system captures these particles to reduce their emissions. Table 5 presents the PM and particulate number (PN) emissions at each condition under WHSC conditions after the installation of the aftertreatment system. With the aftertreatment system, PM emissions at all operating points in the exhaust are nearly zero, with the highest PM emission being only 0.0007 g/(kW·h). It is noteworthy that the full-load range is the primary source of PM emissions in the WHSC test, accounting for 72.8% of the total PM emissions. In contrast, PN emissions exhibit an opposite pattern. In the WHSC conditions, PN emissions in the full-load range account for only 35.8% of the total emissions, while PN emissions in other load ranges account for 64.2%. By comparing PM and PN emissions, it can be concluded that in the main operating range of the ammonia-diesel multi-cylinder engine under steady-state conditions, particulate emissions in the medium-to-low load range primarily consist of smaller particles. These load ranges have relatively lower particle mass emissions but a higher number of particles. In the full-load range, particulate emissions are dominated by larger particles, characterized by fewer particles but a significantly larger mass per particle compared to other load conditions. This distinction between PM and PN emissions highlights the different particle sizes and behaviors at varying engine loads, with the full-load range contributing the most to particulate mass, while medium-to-low loads lead to a higher number of smaller particles.

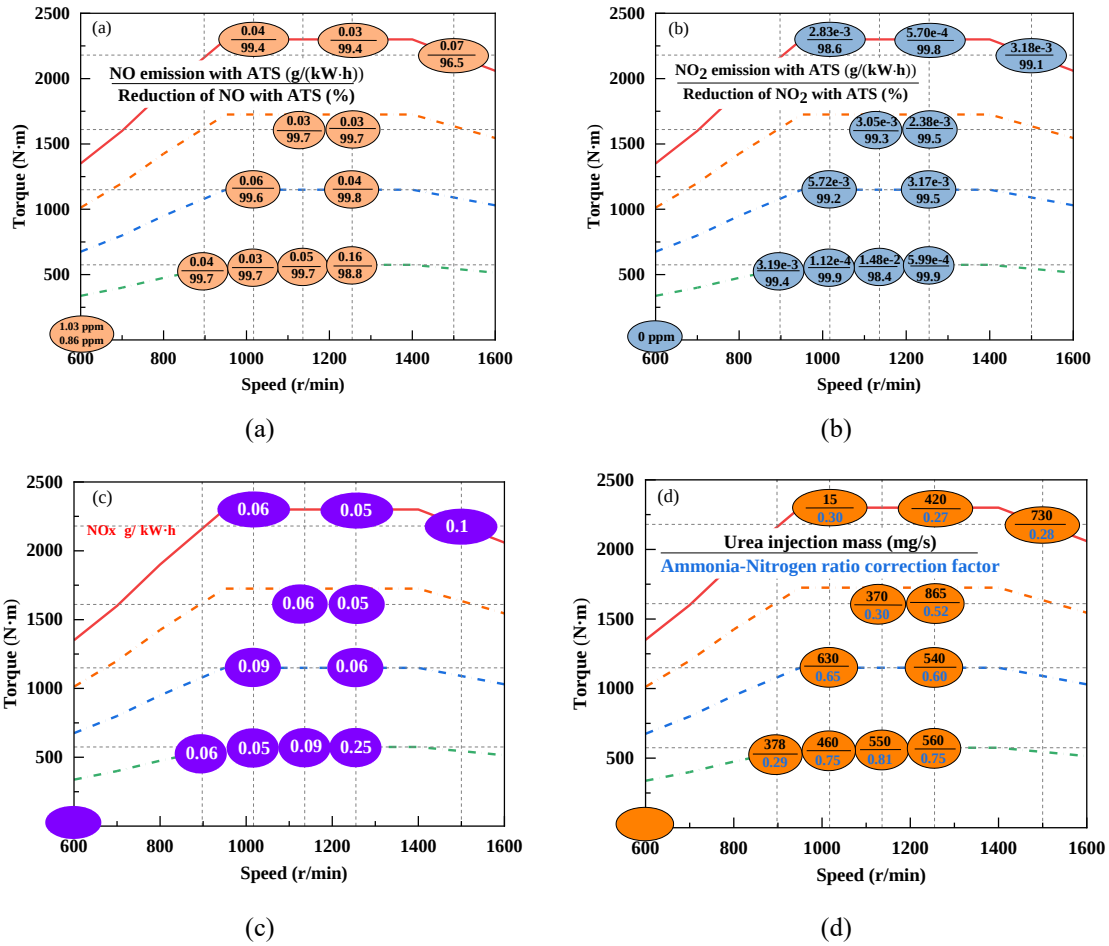

Fig. 14 The emissions comparison of (a) NO and (b) NO2 raw and aftertreatment, (c) NOx at outlet of aftertreatment and (d) urea injection strategies

Table 6 compares the aftertreatment emissions results for the ammonia-diesel multi-cylinder engine with the National VI (China VI) emission standard limits. Through the coordinated optimization of the air system, combustion system, and aftertreatment system, the emissions of various pollutants from the ammonia-diesel engine have been reduced to levels below the National VI regulatory limits. Among the pollutants of primary concern for the ammonia-diesel engine, NOx and ammonia emissions are notably reduced. The NOx emissions are 77.8% lower than the National VI standard limit, while ammonia emissions are reduced by 93.8%. This substantial reduction in emissions demonstrates the effectiveness of the integrated optimization approach in ensuring that the ammonia-diesel engine complies with stringent emissions regulations while maintaining high performance.

Table 5 PM and PN emission at aftertreatment system outlet under WHSC

Operating conditions	Speed r/min	Torque N·m	Running times	PM mg/m^3	PM g/(kW·h)	PM %	PN #/cc	PN #/(kW·h)	PN / %
1	600	0	210	0.01	-	0.6%	2.0×10^{6}	-	5.4%
2	1255	2300	50	-	0.0002	12.6%	-	5.2×10^{8}	2.0%
3	1255	575	250	-	0.0001	2.3%	-	1.2×10^{10}	11.4%
4	1255	1610	75	-	0.0001	2.9%	-	4.8×10^{9}	12.7%
5	1017	2300	50	-	0.0001	6.1%	-	5.0×10^{9}	15.5%
6	898	561	200	-	0.0002	2.4%	-	1.0×10^{10}	6.6%
7	1136	1610	75	-	0.0001	4.1%	-	4.0×10^{9}	9.6%
8	1136	575	150	-	0.0003	4.1%	-	3.3×10^{9}	2.8%
9	1255	1150	125	-	0.0002	5.5%	-	4.8×10^{8}	0.9%
10	1493	2188	50	-	0.0007	54.1%	-	4.3×10^{9}	18.3%
11	1017	1150	200	-	0.0001	2.4%	-	4.6×10^{9}	7.1%
12	1017	575	250	-	0.0001	2.1%	-	3.2×10^{9}	2.5%
13	600	0	210	0.02	-	1.0%	2.0×10^{6}	-	5.4%
WHSC PM emission at ATS outlet g/(kW·h)							0.005		
WHSC PN emission at ATS outlet #/(kW·h)							8.7×10^{10}		

Table 6 The emissions of amonia diesel dual engine operating with WHSC

Emissions	China VI Limits of WHSC	WHSC emissions at ATS outlet
CO g/(kW·h)	1.500	0.003
THC g/(kW·h)	0.130	0.011
NO_x g/(kW·h)	0.400	0.089
NH_3 ppm	10	0.62
PM g/(kW·h)	0.010	0.005
PN #/(kW·h)	8.0×10^{11}	8.7×10^{10}

3.4 The transient experiments research

Based on the previous research, transient WHTC tests were conducted. Since the optimization of ammonia energy replacement ratio and diesel injection strategy across the full operating range was mainly based on steady-state tests, this section of the WHTC focuses on the research of cycle-specific ammonia energy replacement ratio and aftertreatment urea injection strategies, aimed at ensuring the ammonia-diesel engine's exhaust emissions meet the current National VI (China VI) emission standards. This approach helps optimize the engine's transient performance and pollutant emissions, ensuring compliance with stringent regulatory requirements while maintaining the

operational benefits of ammonia-diesel dual-fuel technology.

The validity of the WHTC test results primarily depends on the regression analysis of engine speed and torque. Table 7 shows the results of the regression analysis of engine speed and torque from multiple ADDF engine WHTC tests. Figures 13 and 14 display the speed and torque follow-up curves during the cycle process. The linear regression for speed is generally around 0.97, with a few cycles slightly below this value. The linear regression results for torque are higher, around 0.92, with the lowest value being 0.846. These values generally meet the minimum linear regression limits required for WHTC regarding speed and torque.

The ammonia energy replacement rates for WHTC cycles 5, 6, and 7 are 51.55%, 52.96%, and 52.03%, respectively. These values are somewhat lower compared to the higher ammonia energy replacement ratio observed in WHSC tests. This difference is mainly due to the limited in-cylinder mixture reactivity in the low-load range of the ADDF engine, which results in a lower ammonia energy replacement ratio during the WHTC cycles. Figures 13 and 14 also show some instances of poor torque tracking, particularly during rapid increases in torque around 400s, 500s, and 700s. This is a key factor contributing to the lower regression results for torque (below 0.9). Around 1700s, there are significant fluctuations in both engine speed and torque. This is primarily because this operating point corresponds to the high-speed, low-torque region, where the in-cylinder thermal environment is poor, total fuel injection is low, and mixture reactivity is weak. These factors lead to unstable combustion and large fluctuations in the cycle. Similar issues can be observed in other comparable operating conditions. This analysis highlights the challenges in achieving stable and efficient operation in low-load and high-speed regimes, and the importance of addressing in-cylinder mixture reactivity and thermal conditions for improving the performance of ADDF engines in transient operating conditions.

Table 7 Regression analysis of WHTC

Coefficient	Speed		Torque	
	Lower Limit	Experiment Data	Lower Limit	Experiment Data
WHTC 1	0.97	0.977	0.85	0.858
WHTC 2	0.97	0.974	0.85	0.896
WHTC 3	0.97	0.975	0.85	0.887
WHTC 4	0.97	0.963	0.85	0.846
WHTC 5	0.97	0.976	0.85	0.873
WHTC 6	0.97	0.966	0.85	0.898
WHTC 7	0.97	0.973	0.85	0.889

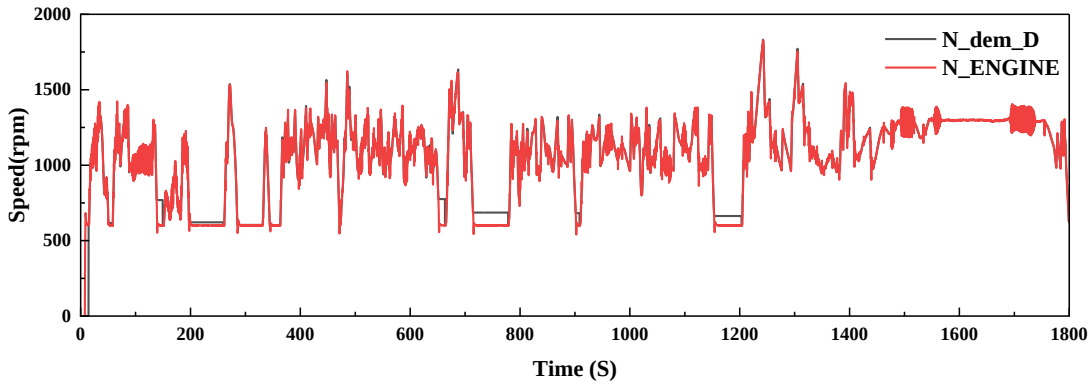

Fig.13 Typical speed-following curve of ADDF engine

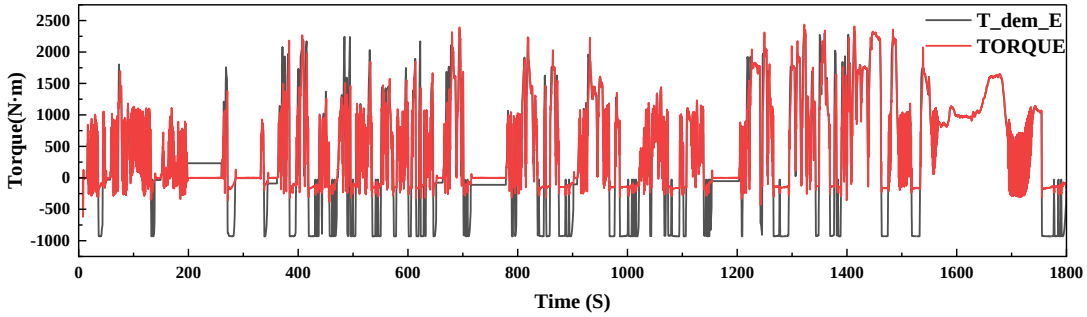

Fig. 14 图 14 Typical torque-following curve of ADDF engine

3.5 The emissions of transient experiments

Due to the reduction in carbon-based fuels in ammonia-diesel engines, emissions of both soot and particulate matter decrease to varying extents as the ammonia energy replacement rate increases. As a result, traditional DPF modules are sufficient to handle these emissions. According to steady-state test results, ammonia-diesel engine exhaust gases contain large amounts of NH_3 and NOx across the full operating range. The traditional SCR system mainly reduces NOx by injecting an aqueous urea solution into the aftertreatment system. The urea decomposes under heat to produce ammonia, which adsorbs onto the active sites of the SCR catalyst, thereby catalyzing the conversion of NOx into harmless N_2 and H_2O. However, due to the large amounts of NH_3 in the exhaust of ammonia-diesel engines, and the varying molar concentration ratios of NH_3 to NOx at different engine speeds and loads, the urea injection strategy of the aftertreatment system becomes crucial for meeting the stringent National VI (China VI) emission standards, especially the strict NH_3 concentration limit, which is set at a maximum of 10 ppm. The complexity of managing NH_3 and NOx emissions in ammonia-diesel engines requires precise control over the urea injection strategy to ensure compliance with these regulations while maintaining optimal engine performance.

Figure 15 illustrates the changes in major pollutants after the aftertreatment system during multiple WHTC tests on the ADDF engine. During the WHTC tests, the impact of the ammonia-to-nitrogen ratio on the pollutant emissions from the aftertreatment system was explored. In the WHTC 1 to WHTC 3 tests, the ammonia-to-nitrogen ratio was increased to some extent, which caused a rise in NH_3 emissions. As shown in Table 8, NH_3 emissions increased from 575 ppm to 761 ppm, while NO emissions decreased from 0.09 g/(kW·h) to 0.04 g/(kW·h). In the WHTC 3 to WHTC 5 tests, the ammonia-to-nitrogen ratio was gradually decreased, resulting in a reduction of NH_3 emissions from 761 ppm (in WHTC 3) to 215 ppm (in WHTC 5). During this period, NO emissions dropped to a minimum value of 0.007 g/(kW·h). This suggests that the NH_3 generated from the thermal decomposition of the injected urea solution in the aftertreatment system, combined with the NH_3 present in the exhaust gases, was more than sufficient to reduce NO emissions. This observation is consistent with the composition of the aftertreatment system, as the final stage in the system is an ASC, which still allowed a significant amount of NH_3 to remain in the exhaust, indicating that the NH_3 concentration in the exhaust gas exceeded the SCR's maximum ammonia storage capacity and the absorption capacity of the ASC, preventing further absorption of NH_3. As a result, in the WHTC 6 test, the urea injection was shut off, and the test showed a significant decrease in NH_3 concentration to 10.2 ppm, while NO emissions only slightly increased to 0.15 g/(kW·h). This confirmed the correctness of the previous strategy, indicating that the original NH_3 concentration in the exhaust was still too high. The NH_3 concentration during WHTC 6 was primarily high in the low-load region at the initial stage and in the high-load region after 1500 seconds. Based on the earlier performance and steady-state test results, it was evident that the ammonia-diesel engine had two regions with excessively high original NH_3 concentrations—one in the high-load region and another in the low-load region.

To address this, the ammonia replacement ratio in these two regions was slightly adjusted before conducting the WHTC 7 test to suppress the original NH_3 concentration. The results of WHTC 7 showed that the NH_3 emissions during the cycle were 7.2 ppm, which is below the National VI emission limit, while NO emissions were only 0.13 g/(kW·h), well below the National VI regulation limit of 0.46 g/(kW·h). This demonstrates the effectiveness of the adjusted ammonia-to-nitrogen ratio strategy in achieving the emission standards.

From Figure 15, it can be observed that NO_2 emissions throughout the entire WHTC cycle remain at relatively low levels. However, N_2O, which plays a dominant role in greenhouse gas effects, shows three distinct peak values, which are relatively high. This is somewhat different from the steady-state test results. To facilitate further discussion, we define a parameter called the **Total**$_{NH3\ mass}$, representing the total NH_3 mass flow rate after the aftertreatment system in a single complete WHTC cycle. From Figure 15, it can be seen that the first peak at around 720 seconds generally increases as the **Total**$_{NH3\ mass}$ decreases across the entire system. This value rises from 1842 ppm in WHTC 3 to 2314 ppm in WHTC 6. The second peak, occurring around 1280 seconds, remains stable at approximately 1000 ppm, showing minimal influence from the **Total**$_{NH3\ mass}$. However, the third peak, around 1320 seconds, shows a significant decrease in NH_3 concentration from nearly 4000 ppm in WHTC 1 to about 2000 ppm in WHTC 7.

As shown in Figure 10, the maximum N_2O emission value across the entire operating range is 1.28 g/(kW·h), corresponding to a concentration of approximately 130 ppm. Therefore, the N_2O in the exhaust gases consists of two main components: one originating from the original exhaust (pre-treatment), and the other generated by the aftertreatment system. After the addition of the aftertreatment system, N_2O peak values increase significantly during transient emissions. This indicates that the overall increase in N_2O emissions during transient cycles is linked to both the original exhaust composition and the interaction between the exhaust gases and the aftertreatment process. The adjustment of NH_3 mass flow in the aftertreatment system, especially in relation to urea injection and ammonia-to-nitrogen ratios, plays a significant role in influencing the peak N_2O emissions.

For WHTC 1 to WHTC 5, NH_3 emissions are mainly concentrated in the initial 100 seconds and between 1200-1400 seconds. This is primarily due to the low initial temperature of the aftertreatment system, which limits the NH_3 handling capability of both the SCR and ASC. Between 1200 and 1400 seconds, the emissions are mainly due to the engine operating in the high-load region. In this region, the NH_3 emissions from the engine are higher, and with the increase in exhaust temperature, the ammonia storage capacity of the SCR decreases[45], leading to increased NH_3 emissions after the aftertreatment system.

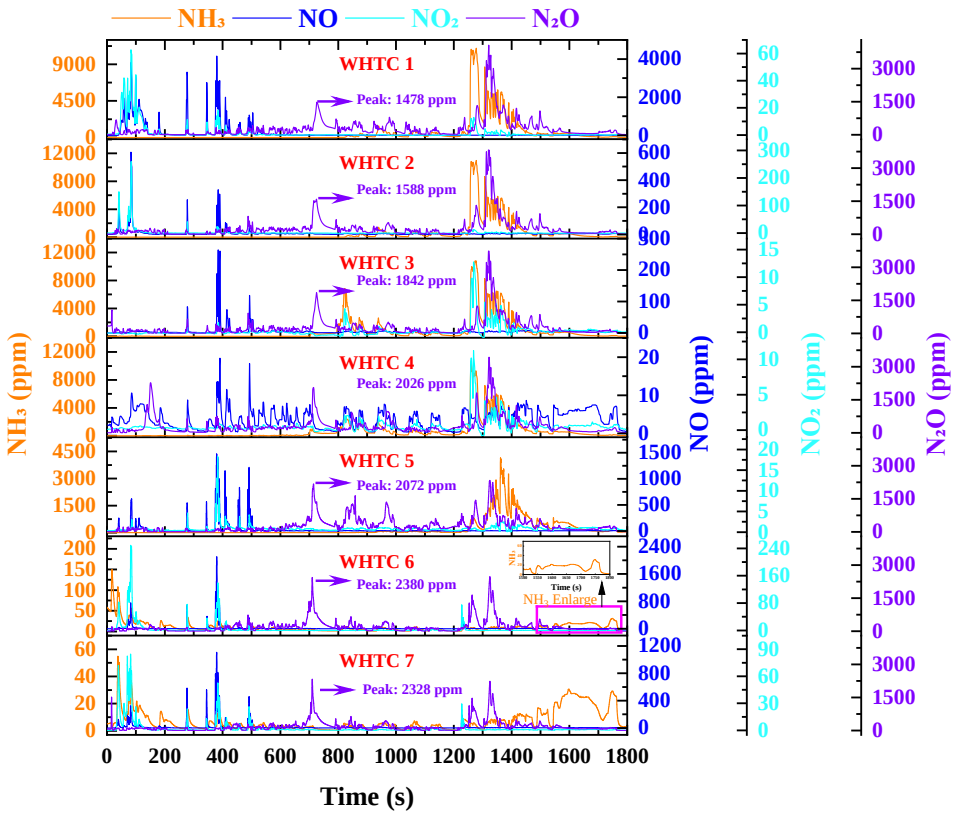

Fig. 15 The transient changes of main pollutants at ATS outlet of ADDF engine under WHTC conditions

Table 8 Emissions results at ATS outlet under WHTC

Case	NH_3 ppm	NO g/(kW • h)	NO_2 g/(kW • h)	NOx g/(kW • h)	N_2O g/(kW • h)	CO g/(kW • h)	CO_2 g/(kW • h)	CH_4 g/(kW • h)
WHTC 1	575	0.09	0.02	0.12	3.6	1.3	201	0.007
WHTC 2	518	0.08	0.02	0.11	3.3	0.04	208	0.007
WHTC 3	761	0.04	0.004	0.07	3.2	0.1	206	0.008
WHTC 4	691	0.03	0.007	0.05	3.5	0.02	208	0.004
WHTC 5	215	0.22	0.01	0.33	3.3	0.02	232	0.002
WHTC 6	10.2	0.15	0.05	0.28	2.5	0.018	224	0.002
WHTC 7	7.2	0.13	0.03	0.22	2.5	0.016	232	0.004

4 Conclusions

This study, based on bench tests, first investigated the influence of ammonia substitution rate, diesel injection strategies (such as pre-injection timing, pre-injection amount, injection pressure, etc.) on the BTE and emission characteristics of multi-cylinder ADDF engines. Based on these findings, the study conducted WHSC performance and emissions optimization, and finally carried out WHTC tests to meet the current National VI emission standards, providing strong support for the commercialization of ADDF engines. The main conclusions of this study are as follows:

1) When using single diesel injection, the original NH_3 escape in the exhaust is as high as 56.82 g/(kW·h). By adopting dual injection and adjusting the proportion of pre-injection diesel and pre-injection timing, the NH_3 escape from the exhaust can be effectively reduced, while the original NOx emissions only increase slightly. However, the maximum in-cylinder peak pressure is significantly

higher compared to the original engine. Therefore, for operating conditions exceeding 70% load, as the pre-injection amount decreases, the injection timing also needs to be appropriately delayed. At full-load conditions, due to the limitation of the maximum in-cylinder peak pressure, this combustion mode cannot be used.

2) Under the optimization logic of WHSC conditions with minimal loss of fuel economy and only a slight increase in original pollutant emissions, the maximum ammonia energy replacement rate can reach 69%. Except for idle conditions, the ammonia energy replacement rate for all other operating points exceeds 50%. At 70% load, the ADDF engine achieves a maximum thermal efficiency that is more than 3% higher than the original engine, reaching 48.8%.

3) After the installation of the aftertreatment system, the engine's maximum BTE decreased to 48.69%. The CO and HC emissions from the aftertreatment system are 0.003 g/(kW·h) and 0.011 g/(kW·h), respectively. NH3 emissions significantly reduced, with the highest point occurring at the operating condition of 2188 Nm @ 1493 r/min, where the concentration was only 2.29 ppm. Given that ammonia is present in the original exhaust, the aftertreatment system should reduce the urea injection amount. Compared to the original engine, the ammonia-to-nitrogen ratio should be controlled below 0.8 in the 25% to 70% load range. The overall NOx emissions in the WHSC are only 0.089 g/(kW·h). PM emissions are 0.0005 g/(kW·h), and PN emissions are 8.7×10^{10} #/(kW·h), mainly concentrated in high-speed, high-load operating conditions.

4) The highest ammonia substitution ratio in the WHTC cycle is 52.96%, mainly due to the lower ammonia substitution rate in the mid-to-low load range of the WHTC cycle. The NH3 emissions after WHTC treatment decrease as the ammonia-to-nitrogen ratio decreases. When the cycle urea injection amount is zero, the NH3 emissions are 7.2 ppm. Additionally, ammonia emissions are concentrated in the initial low-temperature state of the post-treatment system and the high-load range between 1500 s and 1700 s. The N2O in the exhaust is generated from two sources: one is produced during the engine's combustion process, and the other is produced by the post-treatment system.

5 Acknowledgements

This work has been funded by National Key Research and Development Program of China(2024YFE0213200) and the High-tech ship research projects “Key technologies research for ammonia-fueled marine engines based on the Otto cycle.

6 REFERENCES AND BIBLIOGRAPHY

[1] Hannah Ritchie, Roser M, Rosado P. CO_2 and Greenhouse Gas Emissions[Z]. Published online at OurWorldInDataorg Retrieved from: 'https://ourworldindataorg/co2-and-greenhouse-gas-emissions'. 2020

[2] Aizebeokhai A P. Global warning and climate change: Realities, uncertainties and measures[J]. International Journal of physical sciences, 2009, 4(13): 868-879.

[3] Towoju O A, Ishola F A. A case for the internal combustion engine powered vehicle[J]. Energy Reports, 2020, 6: 315-321.

[4] Gunfaus M T, Waisman H. Assessing the adequacy of the global response to the Paris Agreement: Toward a full appraisal of climate ambition and action[J]. Earth System Governance, 2021, 8: 100102.

[5] Huang M-T, Zhai P-M. Achieving Paris Agreement temperature goals requires carbon neutrality by middle century with far-reaching transitions in the whole society[J]. Advances in Climate Change Research, 2021, 12(2): 281-286.

[6] Chu H, Qi J, Feng S, et al. Soot formation in high-pressure combustion: Status and challenges[J]. Fuel, 2023, 345: 128236.

[7] Hegab A, Dahuwa K, Islam R, et al. Plasma electrolytic oxidation thermal barrier coating for reduced heat losses in IC engines[J]. Applied Thermal Engineering, 2021, 196: 117316.
[8] Cardoso J S, Silva V, Rocha R C, et al. Ammonia as an energy vector: Current and future prospects for low-carbon fuel applications in internal combustion engines[J]. Journal of Cleaner Production, 2021, 296: 126562.
[9] Epa G G E. Global Greenhouse Gas Overview[Z]. Published online at Environmental Protection Agency Retrieved from: 'https://ourworldindataorg/co2-and-greenhouse-gas-emissions'. Retrieved on 28/08/2024
[10] Olivier J G J, Peters J a H W. TRENDS IN GLOBAL CO2 AND TOTAL GREENHOUSE GAS EMISSIONS, F, 2019 [C].
[11] Shi M, Jin S, Wang J, et al. Structural optimization study of ammonia-diesel dual-fuel engine based on reactivity turbulent jet disturbance coupled aerodynamics under high load conditions[J]. Applied Thermal Engineering, 2024, 256: 124133.
[12] Ma X, Wang Q, Xiong S, et al. Application of fuel cell and alternative fuel for the decarbonization of China's road freight sector towards carbon neutral[J]. International Journal of Hydrogen Energy, 2024, 49: 263-275.
[13] Zhao P, Zeng L, Li P, et al. China's transportation sector carbon dioxide emissions efficiency and its influencing factors based on the EBM DEA model with undesirable outputs and spatial Durbin model[J]. Energy, 2022, 238: 121934.
[14] Bae C, Kim J. Alternative fuels for internal combustion engines[J]. Proceedings of the Combustion Institute, 2017, 36(3): 3389-3413.
[15] Society T R. Ammonia: Zero-Carbon Fertiliser[Z]. Fuel and Energy Store. London, U.K.; The Royal Society. 2020
[16] Brown T. Updating the literature: Ammonia comsumes 43% of global hydrogen[Z]. 2020
[17] Sonker M, Tiwary S K, Shreyash N, et al. Ammonia as an alternative fuel for vehicular applications: Paving the way for adsorbed ammonia and direct ammonia fuel cells[J]. Journal of Cleaner Production, 2022, 376: 133960.
[18] Valera-Medina A, Amer-Hatem F, Azad A K, et al. Review on Ammonia as a Potential Fuel: From Synthesis to Economics[J]. Energy & Fuels, 2021, 35(9): 6964-7029.
[19] Ishaq H, Crawford C. Review of ammonia production and utilization: Enabling clean energy transition and net-zero climate targets[J]. Energy Conversion and Management, 2024, 300: 117869.
[20] Xiang P, Jiang K, Wang J, et al. Zero-carbon ammonia technology pathway analysis by IPAC-technology model in China[J]. Journal of Cleaner Production, 2023, 400: 136652.
[21] Kurien C, Mittal M. Review on the production and utilization of green ammonia as an alternate fuel in dual-fuel compression ignition engines[J]. Energy Conversion and Management, 2022, 251: 114990.
[22] Yousefi A, Guo H, Dev S, et al. Effects of ammonia energy fraction and diesel injection timing on combustion and emissions of an ammonia/diesel dual-fuel engine[J]. Fuel, 2022, 314: 122723.
[23] Nadimi E, Przybyła G, Lewandowski M T, et al. Effects of ammonia on combustion, emissions, and performance of the ammonia/diesel dual-fuel compression ignition engine[J]. Journal of the Energy Institute, 2023, 107: 101158.
[24] Kobayashi H, Hayakawa A, Somarathne K D Kunkuma a, et al. Science and technology of ammonia combustion[J]. Proceedings of the Combustion Institute, 2019, 37(1): 109-133.
[25] Varea E, Modica V, Vandel A, et al. Measurement of laminar burning velocity and Markstein length relative to fresh gases using a new postprocessing procedure: Application to laminar spherical flames for methane, ethanol and isooctane/air mixtures[J]. Combustion and Flame, 2012, 159(2): 577-590.
[26] Takizawa K, Takahashi A, Tokuhashi K, et al. Burning velocity measurements of nitrogen-containing compounds[J]. Journal of Hazardous Materials, 2008, 155(1): 144-152.
[27] Law C K. Combustion Physics[M]. Cambridge University Press, 2010.
[28] Pfahl U J, Ross M C, Shepherd J E, et al. Flammability limits, ignition energy, and flame speeds in H2–CH4–NH3–N2O–O2–N2 mixtures[J]. Combustion and Flame, 2000, 123(1): 140-158.

[29] Hayakawa A, Goto T, Mimoto R, et al. Laminar burning velocity and Markstein length of ammonia/air premixed flames at various pressures[J]. Fuel, 2015, 159: 98-106.
[30] Ronney P D. Effect of Chemistry and Transport Properties on Near-Limit Flames at Microgravity[J]. Combustion Science and Technology, 1988.
[31] Yang P, Luo Y, Jin S, et al. Study on the effect of turbulent jet combustion chamber on combustion characteristics at different ammonia energy ratio and optimization of an ammonia-diesel dual-fuel engine[J]. Journal of the Energy Institute, 2024, 112: 101431.
[32] Wu B, Shi M, Jin S, et al. Comparison and optimization of strategies for ammonia-diesel dual-fuel engine based on reactivity assisted jet ignition and reactivity turbulent jet disturbance under high load conditions[J]. International Journal of Hydrogen Energy, 2024, 67: 487-499.
[33] Mi S, Zhang J, Shi Z, et al. Optimization of direct-injection ammonia-diesel dual-fuel combustion under low load and higher ammonia energy ratios[J]. Fuel, 2024, 375: 132611.
[34] Bjørgen K O P, Emberson D R, Løvås T. Combustion of liquid ammonia and diesel in a compression ignition engine operated in high-pressure dual fuel mode[J]. Fuel, 2024, 360: 130269.
[35] Jin S, Wu B, Zi Z, et al. Effects of fuel injection strategy and ammonia energy ratio on combustion and emissions of ammonia-diesel dual-fuel engine[J]. Fuel, 2023, 341: 127668.
[36] Wu B, Zi Z, Jin S, et al. Effect of Diesel Injection Strategy and Ammonia Energy Fraction on Ammonia-Diesel Premixed-Charge Compression Ignition Combustion and Emissions[J]. Fuel, 2024, 357: 129785.
[37] Pei Y, Wang D, Jin S, et al. A quantitative study on the combustion and emission characteristics of an Ammonia-Diesel Dual-fuel (ADDF) engine[J]. Fuel Processing Technology, 2023, 250: 107906.
[38] Wang X, Shi T, Jin S, et al. Effects of different ammonia energy ratio on soot formation and oxidation in an ammonia diesel dual-fuel engine[J]. Science of The Total Environment, 2024, 946: 174096.
[39] Shin J, Park S. Numerical analysis for optimizing combustion strategy in an ammonia-diesel dual-fuel engine[J]. Energy Conversion and Management, 2023, 284: 116980.
[40] Liu J, Wang X, Zhao W, et al. Effects of ammonia energy fraction and diesel injection parameters on combustion stability and GHG emissions characteristics in a low-loaded ammonia/diesel dual-fuel engine[J]. Fuel, 2024, 360: 130544.
[41] Jamrozik A, Tutak W, Pyrc M, et al. Experimental study on ammonia-diesel co-combustion in a dual-fuel compression ignition engine[J]. Journal of the Energy Institute, 2024, 115: 101711.
[42] Wang X, Li T, Chen R, et al. Exploring the GHG reduction potential of pilot diesel-ignited ammonia engines - Effects of diesel injection timing and ammonia energetic ratio[J]. Applied Energy, 2024, 357: 122437.
[43] Jin S, Zi Z, Yang P, et al. The influence of exhaust gas recirculation on combustion and emission characteristics of ammonia-diesel dual-fuel engines: Heat capacity, dilution and chemical effects[J]. Journal of the Energy Institute, 2024, 117: 101778.
[44] Wu B, Wang Y, Wang D, et al. Generation mechanism and emission characteristics of N2O and NOx in ammonia-diesel dual-fuel engine[J]. Energy, 2023, 284: 129291.
[45] Wu B, Deng L, Liu Y, et al. Urea injection control strategy in urea-selective catalytic reduction for heavy-duty diesel engine under transient process[J]. 2021, 22(2): 516-527.